WattsWorth: Monitor Electric Power Anywhere

John Donnal, *Student Member, IEEE,* Steven B. Leeb, *Fellow, IEEE*

***Abstract*—Energy monitoring and control strategies can be asymmetrical, chasing pennies of hoped-for savings with dollars of installation and monitoring expense. Modern sensors can be used to accurately measure voltage and current without the requirement for a permeable magnetic core or the need to surround the conductor, e.g., with a Rogowski coil. These sensors can be used to find currents and voltages without the need to invasively separate existing conductors. These sensors could greatly lower installation and monitoring expense, and provide quickly installed access for acquiring actionable energy consumption information and power quality assessment.**

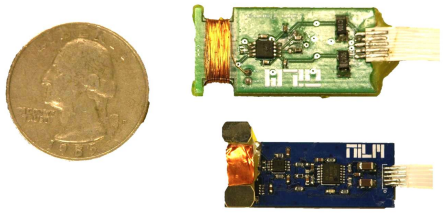

Fig. 1. WattsWorth Sensors: TMR-based (top) Hall Effect-based (bottom)

I. Introduction

Appliances, electronics, and lighting account for nearly 35% of residential power consumption [1]. Power electronics and power electronic controls are increasingly prevalent in these loads. While the types and uses of power electronics have increased significantly, the ability to monitor consumption has not improved in many respects. Monthly power bills do not communicate the time varying cost of electric power generation and do not provide feedback on how much particular appliances consume. Diagnostics from electrical signals generally involve the installation of intrusive current and voltage sensors, or must be "designed in" during the construction of a drive or similar load.

Recent studies have shown that households with real time energy meters consume an average of 3.8% less power than those with standard meters [2]. A "smart meter" that communicates with the utility enables even more effective cost savings because the utility can dynamically price consumption at the marginal cost of production, encouraging consumers to reduce demand during peak load times [3]. For these reasons, the GO 15, an international organization of the world's largest Power Grid Operators, has prioritized investment in improved power monitoring technology [4]. Unfortunately the financial and logistical difficulties of installing such power meters has limited their adoption by utilities and their customers [3].

Traditional power meters require an electrician to install, or must be built in to a product. WattsWorth offers easier access to electrical consumption information for energy scorekeeping, diagnostics, and control. A non-contact sensor enables power monitoring without direct access to any electrical conductors. Sensors can be placed on the outside of a circuit breaker box, around the service entry cable, or on any electric cord. Installation is easy and does not require a trained electrician or a service interruption. Conductors do not have to be separated, voltage and current can be measured simultaneously, and it is not necessary to geometrically surround conductors completely with any material.

Nonintrusive measurement of electric power requires analog sensors. The design and implementation of these circuits is discussed first. Calculating the power in a single breaker on a panel or in a specific wire of a cable is complicated by the presence of nearby conductors carrying unknown currents and voltages. A reliable method for measuring power in these multi-conductor environments is presented. Finally, a sensor calibration process is described which allows users to arbitrarily place WattsWorth sensors and retrieve accurate power measurements, all without any service interruption.

II. Monitoring Power with WattsWorth

Measuring electric power consumption requires current and voltage sensing. There are many current and voltage sensors available but they generally require significant installation effort. Voltage sensors may involve an ohmic contact. Current sensors often require separated access to each conductor, and may require a wire to be completely surrounded by a material in order to accurately sense current. In many environments these requirements are prohibitive. WattsWorth sensors do not require ohmic contact or access to isolated conductors. This greatly reduces the burden of installation and makes it easy to assess consumption.

WattsWorth sensors do not require any service interruption to install. In environments with high "up time" requirements and mission critical equipment, retrofitting power monitors has proven challenging. For example, military forward operating bases (FOB's) rely on generators and therefore have a vested interest in monitoring power consumption. However, electrical requirements change quickly as tenant units add and remove equipment depending on their particular mission. Figure 2 shows a model FOB at Fort Devens, MA where Army technicians evaluate power monitoring technologies. Requiring an electrician to disconnect all power and install sensors each time new equipment is added or removed from the FOB is not a feasible solution. With WattsWorth, any power cable or breaker panel can become a power monitoring node and when a cable or panel is no longer a target of interest, the sensors can be easily moved to a new location.

WattsWorth current and voltage sensors have sufficient bandwidth to resolve the high order harmonics that characterize many power electronic devices and motors. Figure 3 shows WattsWorth measurements for three different loads.

978-1-4799-2325-0/14/$31.00 ©2014 IEEE

Fig. 2. Ad-hoc power distribution network at Fort Devens, MA

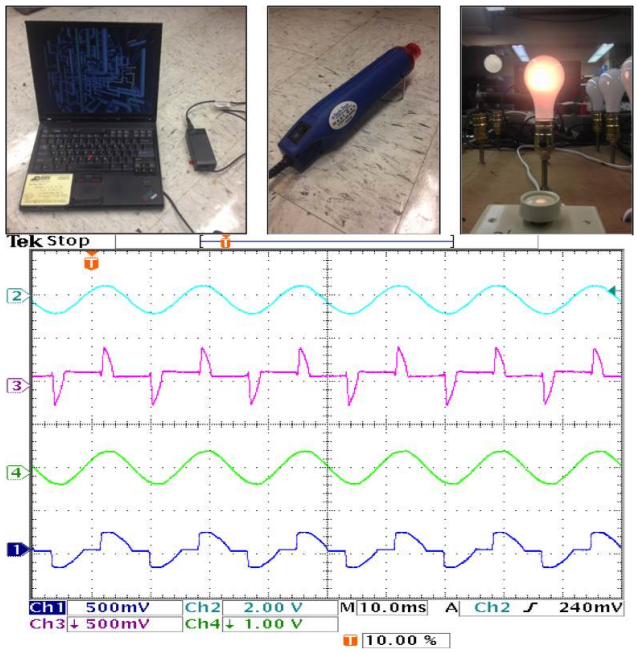

Fig. 3. Measuring common electric loads with WattsWorth sensors.

The top trace is voltage which is common to all the loads. The second trace is an IBM Think Pad which, like many consumer-grade power chargers, draws current pulses. The third trace is a heat gun which, as a purely resistive load, is a relatively sinusoidal waveform. The final load is a lightbulb on a phase controlled dimmer. These three exemplars illustrate the variety of current draw in common electric loads and suggest exciting identification and diagnostic applications for WattsWorth power monitors for nonintrusive load monitoring.

III. Non-Contact Current Sensing

One of the primary difficulties in non-contact power monitoring is designing a sensor capable of measuring current flow at a distance. Ampere's Law establishes the linear relationship between magnetic fields and current, but without a closed path around the conductor, accurately measuring this field is

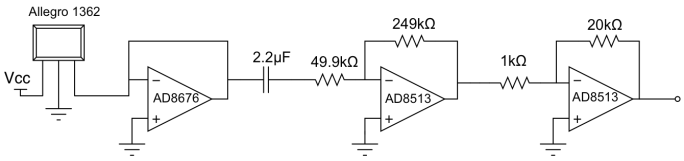

Fig. 4. Schematic of Hall Effect-based current sensor

a challenging task. On the surface of a circuit breaker and the exterior of a power cable, the fields are not uniformly radial, and depending on the particular geometry, can be very small-less than 1 Gauss for bench top load currents in typical wires. Two circuit topologies are introduced that can accurately sense these small fields and can do so even in the presence of DC offsets introduced by nearby magnetic elements such as steel breaker panels, and the Earth itself. Figure 1 shows the fabricated prototypes of both circuits.

The Hall Effect design is a cost effective solution suitable for measuring larger loads or in situations where the wire topology exposes a relatively strong magnetic field. The Tunneling Magnetoresistive (TMR)-based circuit uses a recently introduced sensor technology [5] and an inductive feedback technique to accurately measure extremely small fields. The response of both sensors are evaluated with the experimental setup shown in Figure 5. For illustration and characterization, each sensor was placed in an air core solenoid where a signal generator coupled with a power amplifier generates a magnetic field. Sensor output is compared to the field strength as measured with a fluxgate-magnetometer (an Aim Instrument I-proper 520). Results for the Hall Effect and TMR-based sensors are shown in Figures 6 and 10 respectively. Two levels of field strength illustrate the degree of hysteresis in the sensor response. Steeper slope reflects higher sensitivity.

A. Hall Effect Sensor

The Hall Effect is widely known and used in many current sensor designs. One of the most sensitive devices available in quantity is Allegro MicroSystem's A1362 Hall Effect sensor [6]. The A1362 has a programmable gain which can be set up to 16 mV/G, sufficient to resolve the magnetic fields of interest. The quiescent output level is also programmable but not tightly controlled. Therefore, in order to measure small fields without saturating the output, a high pass filter with a cutoff at 1.5 Hz AC-couples the sensor to the inverting amplifier gain stage. The large capacitive input of the filter stage requires a follower to buffer the sensor output. Overall gain can be adjusted by tuning the feedback leg of the gain stage; however, adding additional amplification to resolve smaller fields is of limited utility because the A1362 has a gain independent noise floor of 8mV.

In situations where the geometry of the fields is approximately known, the response of the Hall Effect circuit can be improved by attaching magnetic material parallel to the field lines around the A1362 chip. The power line in Figure 16 has generally radial fields near each conductor which are focused onto the sensor head by a partial ferrite ring.

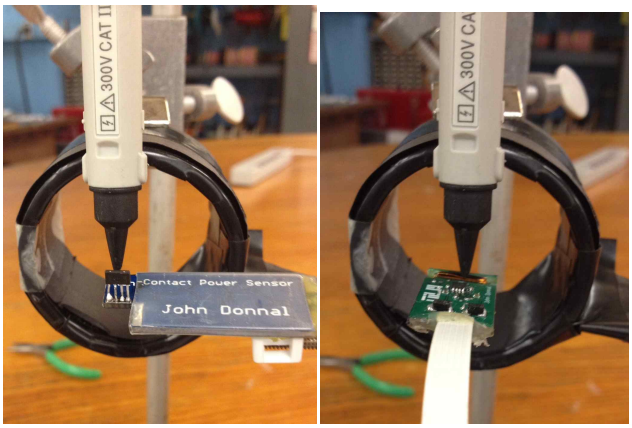

(a) Hall Effect Sensor (b) Compensated TMR Sensor

Fig. 5. Evaluating sensor response in applied magnetic fields

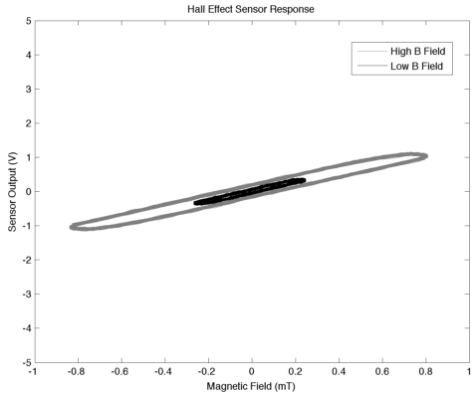

Fig. 6. Response of Hall Effect-based sensor to applied fields

B. Tunneling Magnetoresistive Sensor

The TMR effect describes the change in resistance of a particular material due to applied magnetic fields. An explanation of the effect was first published in the 1970's but garnered little interest because practical implementations generated relatively small changes in material resistance [7] . Recent advancements using new materials and advanced fabrication techniques have improved the sensitivity of TMR devices. Modern state of the art sensors show up to 600% change in relative resistance at room temperature [8], [9]. Interest in these devices has increased as they have become integrated into high density magnetic disk drives and MRAM [10].

The STJ-340 is a TMR Wheatstone bridge sensor produced by MircoMagnetics. The sensor has four active TMR elements, arranged in a Wheatsone bridge architecture. Changes in the field induce an imbalance in the bridge which can be measured by a differential amplifier [5]. While the STJ-340 can detect very small fields (25mV/G as constructed), there are two significant challenges in using it as a current sensor. First, as with the Hall Effect-based sensor, DC offset errors quickly saturate the sensor output. The offset errors from the environment and from imbalance in the bridge itself (which can be up to 10%) must be removed before applying any significant gain to the output. More troubling though is the

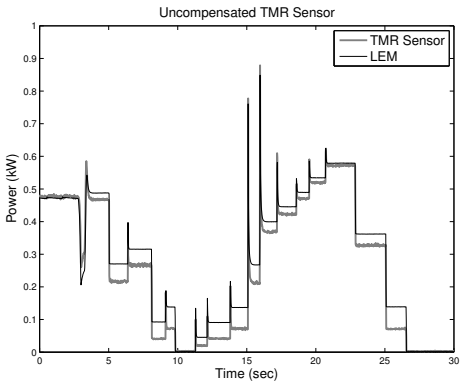

Fig. 7. Non-linear response of an uncompensated TMR-based sensor

sensor's nonlinear response to large changes in the applied field. Figure 7 compares the true current (as measured by a LEM sensor) to the output of a TMR-based sensor. Even with proper amplification and DC offset removal, step changes in the load current produce non-linear responses in the sensor output.

The circuit shown in Figure 8 addresses both the DC offset and the non-linearity problems of the TMR sensor. The DC offset error is corrected by an integrator connected to the REF pin of the instrumentation amplifier. Any DC component is subtracted off the amplifier output resulting in a purely AC signal. This output is then fed through a high gain stage which drives an air core solenoid wrapped around the STJ-340. The current through this solenoid builds a magnetic field that opposes the applied field, creating a feedback loop that zeros the operating point of the STJ-340. Keeping the sensor element exposed to very small fields improves the sensor linearity and increases its range of operation. The current driven in the compensation solenoid is sensed as a voltage across a 150Ω resistor. The final stage is a high pass filter and gain stage that removes any offset not compensated for in the integrator.

The conceptual operation of the feedback topology is shown in Figure 9. In steady state operation the sensed H_{src} and driven H_{comp} fields are approximately equal and the TMR element is exposed to only a very small residual field. The air core solenoid has proven remarkably effective because closed-loop feedback is used to control the compensation coil. Figure 10 shows the high sensitivity and linear response of the compensated TMR-based sensor.

IV. Non-Contact Voltage Sensing

The voltage in a conductor generates an electric field which radiates to the surface of the cable or breaker panel. By measuring the voltage this field induces on a capacitive pickup, it is possible to calculate the voltage of the conductor itself. The full non-contact voltage sensor schematic is shown in Figure 11. The instrumentation amplifier has two capacitive pickups (copper foil). This creates a differential sensor but the circuit operation is most easily understood by considering a single ended sensor with the negative amplifier input connected to ground. The 1MΩ resistor provides input bias current to the

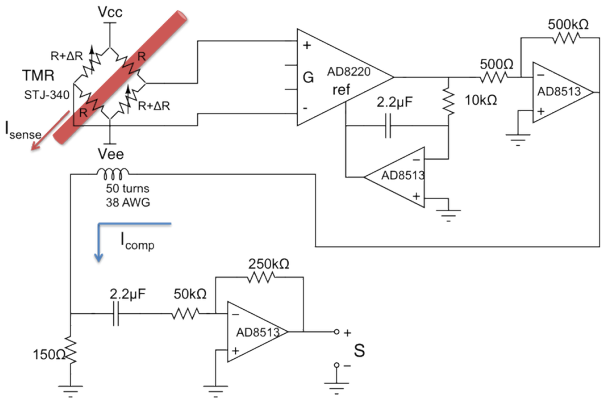

Fig. 8. Schematic of the compensated TMR-based current sensor

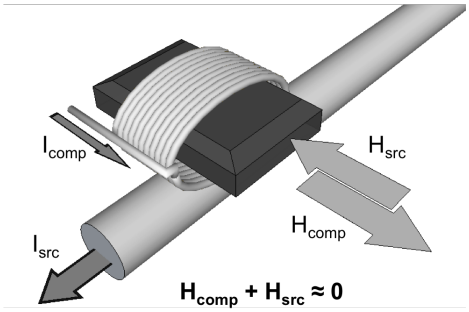

Fig. 9. Illustration of TMR feedback technique

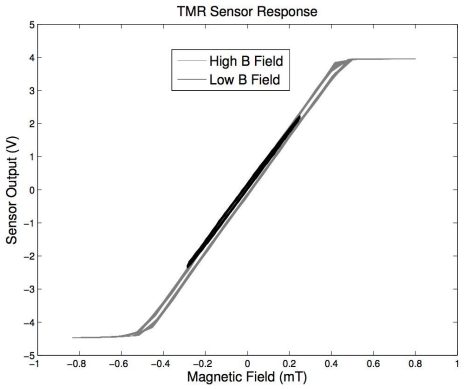

Fig. 10. Response of compensated TMR-based sensor to applied fields

amplifier while maintaing the high impedance required to build up voltage on the pickup due to the surrounding field. This input stage forms an RC divider with a transfer function of

$$H(s) = \frac{sRC}{1 + sRC} \tag{1}$$

While the resistance is high, on the order of the bias resistor, the capacitance is very small, estimated to be on the order of a few picofarads, so the quantity $sRC \ll 1$ and the transfer function reduces to sRC. In order to compensate this undesired frequency response, the instrumentation amplifier is followed by an integrator. As with the non-contact current sensor, any DC offset leads to saturation at the gain stage so a feedback loop similar to the REF pin removes any common

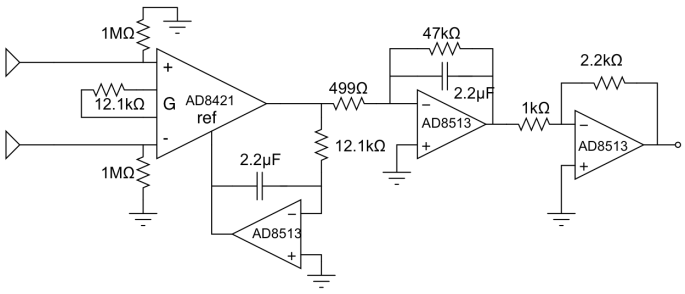

Fig. 11. Non-contact voltage sensor schematic

mode voltage offset between the foil pickups. The final stage is a standard inverting amplifier.

The electric field can be measured using a single ended topology but a differential design increases the performance with minimal increase in complexity. In an environment with many different high voltage conductors, a single foil pickup acts as an omnidirectional sensor. By using a differential setup the sensor can be directionally targeted to the region of interest. Figure 13 illustrates the differential sensor operation. Conductors directly below the sensor generate higher magnitude fields on the bottom plate than on the top plate while conductors to the sides of the sensor generate equal magnitude fields on both plates. The differential amplifier rejects the common mode signals providing selectively higher gain to conductors located below the sensor head.

In addition to increasing the positional sensitivity of the device, the differential input also attenuates the sensitivity to weak fields in the environment. This can be understood by considering the magnitude of the electric field at the sensor plate in terms of charge on the conductor of interest. The electric field is described by Coulomb's law where q is the charge on the conductor and r is the distance from the conductor to the sensor plate:

$$|E| \propto \frac{q}{r^2} \tag{2}$$

For the differential circuit the two plates are stacked vertically, and assuming a unit distance between the plates, the output of the sensor becomes

$$\begin{aligned} S_{diff} &= |E_+| - |E_-| \\ &\propto \frac{q}{r^2} - \frac{q}{(1+r)^2} \end{aligned} \tag{3}$$

Figure 12 shows a logarithmic plot of sensitivity versus distance for the single and differential pickups. The differential topology reduces the pickup of extraneous electric fields which significantly improves sensor operation in environments with unwanted 60Hz pick-up.

V. Monitoring Multiple Conductors

In many systems of interest there are multiple current-carrying conductors. If the magnetic fields of the conductors overlap, the output of any single non-contact sensor will represent a combination of multiple fields and misrepresent the current flowing in the nominal conductor of interest. Figure

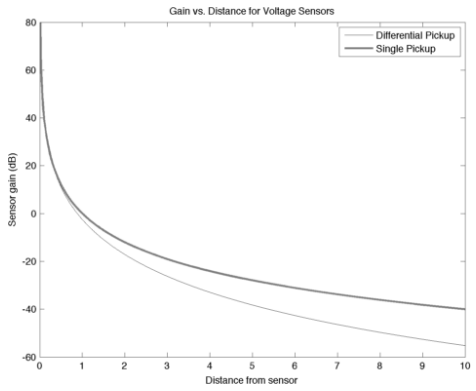

Fig. 12. The differential pickup attenuates distant fields more than a single pickup does, improving the specificity of the non-contact sensor

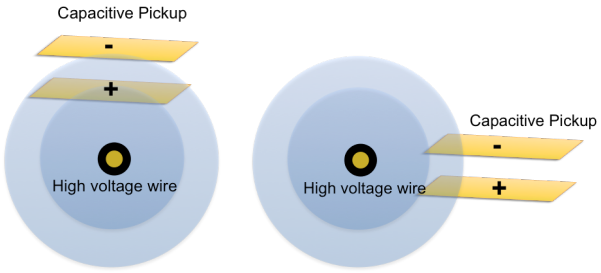

(a) Differential mode (b) Common mode

Fig. 13. Differential design concentrates the gain below the sensor

14 shows the result of non-contact sensing with "open air" sensors over two conductors in close proximity, compared with a conventional LEM sensor accurately measuring single separated feed wires in the panel. Each "open air" sensor picks up significant interference from current in the neighboring conductor The following section introduces techniques for accurately measuring current in environments with complex, superposed magnetic fields.

A. Monitoring a Circuit Breaker Panel

Due to the close proximity of circuits on a breaker panel and the steel construction of the panel itself, the magnetic fields are often fully mixed so that any single sensor detects some portion of every current flowing through the panel or cable. Even if a precise location for minimal interference could be determined, the narrow dimensions of many breaker panels limit placement options as seen in Figure 15. Assuming the breaker currents are linearly independent, N sensors are required to measure N breakers. The n^{th} sensor output for an N breaker panel can be expressed as:

$$S_n = M_1 I_1 + M_2 I_2 + \ldots + M_N I_N \tag{4}$$

Or, equivalently using the inverse relationship, for N sensors, the n^{th} breaker current can be expressed as:

$$I_n = K_1 S_1 + K_2 S_2 + \ldots + K_N S_N \tag{5}$$

The full system can be expressed in matrix form where the current flowing in the breaker directly under each sensor

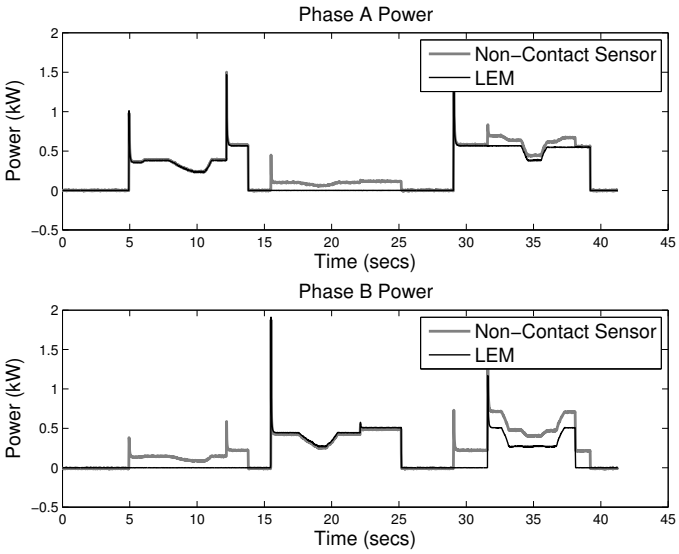

Fig. 14. Interfering magnetic fields corrupt power line measurement

Fig. 15. Monitoring a circuit breaker panel with TMR sensors

is represented by the diagonal K values and the interference terms are the off-diagonal K's.

$$\begin{bmatrix} I_1 \\ I_2 \\ I_3 \\ \vdots \end{bmatrix} = \begin{bmatrix} K_{11} & K_{12} & K_{13} & \\ K_{21} & K_{22} & K_{23} & \ldots \\ K_{31} & K_{32} & K_{33} & \\ & \vdots & & \end{bmatrix} \times \begin{bmatrix} S_1 \\ S_2 \\ S_3 \\ \vdots \end{bmatrix} \tag{6}$$

B. Monitoring Cables with Neutral Return Path

The equations are slightly different for a multiple conductor cable such as the two phase power cable shown in Figure 16. These systems do not have fully independent conductors and are subject to the additional constraint of Kirchoff's Current Law:

$$I_1 + I_2 + I_3 + \ldots + I_{neutral} = 0 \tag{7}$$

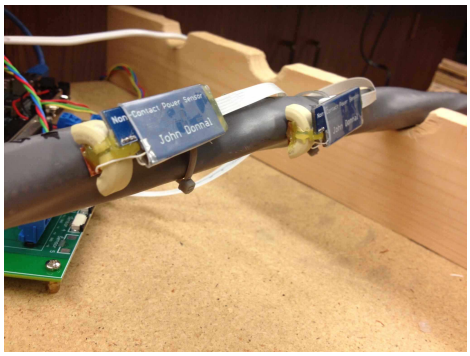

Fig. 16. Monitoring a standard power line with Hall Effect sensors

This equation reduces the dimension of the solution space. Standard power cables have only two current-carrying wires- hot and neutral and in this simple case only a single sensor is needed. The equations to find current are:

$$\begin{aligned} I_{hot} &= KS \\ I_{neutral} &= -I_{hot} \end{aligned} \tag{8}$$

The same technique can be extended for multiple phases and a common neutral. For a three phase power cable there are four current carrying wires so the general matrix has 16 elements but KCL reduces the number of unknown currents by one. A nine element matrix using only three sensors is enough to determine all the currents. The equations for a three phase power cable are:

$$\begin{bmatrix} I_1 \\ I_2 \\ I_3 \end{bmatrix} = \begin{bmatrix} K_{11} & K_{12} & K_{13} \\ K_{21} & K_{22} & K_{23} \\ K_{31} & K_{32} & K_{33} \end{bmatrix} \times \begin{bmatrix} S_1 \\ S_2 \\ S_3 \end{bmatrix} \tag{9}$$

$$I_{neutral} = -(I_1 + I_2 + I_3)$$

Applying the fit matrix with appropriate K values to a system with interfering fields decouples the sensors and provides accurate current measurements for each conductor in the system. Figure 17 shows the same data as Figure 14 after multiplication by the system fit matrix.

VI. System Calibration

Equations (6,8,9) can calculate all currents of interest in complex systems, but they cannot be used until the K values in the fit matrix are determined. If only one current is present, the matrices reduce to a set of equations relating the current to a specific sensor:

$$\begin{bmatrix} S_1 \\ S_2 \\ S_3 \\ \vdots \end{bmatrix} = \begin{bmatrix} M_{11} & M_{12} & M_{13} & \\ M_{21} & M_{22} & M_{23} & \\ M_{31} & M_{32} & M_{33} & \dots \\ & \vdots & & \end{bmatrix} \times \begin{bmatrix} I_1 \\ 0 \\ 0 \\ \vdots \end{bmatrix} \tag{10}$$

$$\Downarrow$$

$$\begin{aligned} S_1 &= M_{11} I_1 \\ S_2 &= M_{21} I_2 \\ S_3 &= M_{31} I_3 \\ \vdots &\quad \vdots \end{aligned}$$

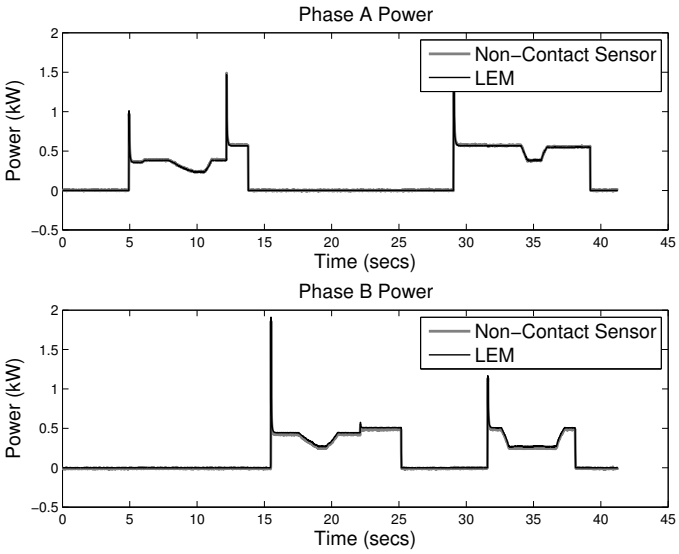

Fig. 17. Fit matrix recovers individual current components

Iterating with a known current on each conductor produces the full matrix $[M]$. The fit matrix can be found as

$$[K] = [M]^{-1} \tag{11}$$

While technically correct, this method places an undue burden on the user to first shut down all connected loads and then connect a single known load to each conductor in sequence. If the system of interest is a circuit breaker panel this type of calibration is unrealistic – a homeowner or facilities manager is unlikely to shut off the power and walk around in the dark connecting test loads. In environments with mission critical equipment, such as a microgrid on an Army FOB, this type of calibration is impossible.

A. Current Sensor Calibration

The approach illustrated here is one example of any number of methods that could use frequency and time coded information to calibrate. One practical calibration procedure can be performed by toggling a known load periodically to generate a square wave envelope in current. If no other loads are present on the circuit, the scaling factor can be found by dividing the height of the measured envelope by the known current draw of the calibration load. Unlike the previous calibration technique however, this procedure can be used when other loads are present in the system and therefore requires no service interruption. Connecting a calibration load to a "live" system is shown in figure 18. Arbitrary loads are active on both phases throughout the calibration sequence complicating the shape of the current envelope. Using the Fourier Transform, however, the calibration signature can be extracted from the signal and used to calculate the parameters of the fit matrix.

The calibration load draws 6.25 amps and is toggled at 3Hz. Extracting the current envelope from the raw sensor output effectively down samples the signal to 60Hz. Using the

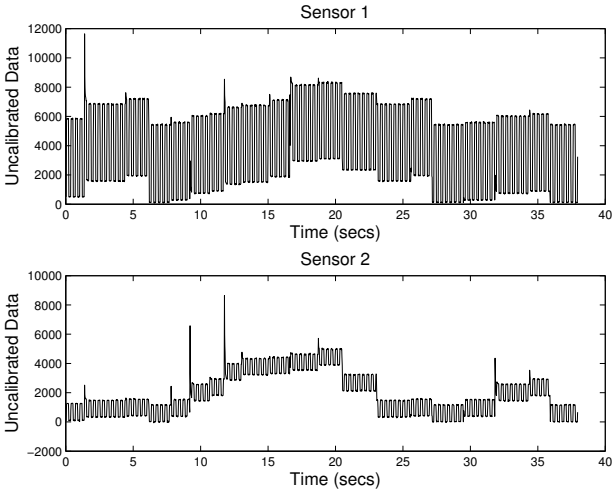

(a) Calibrating load connected to phase A

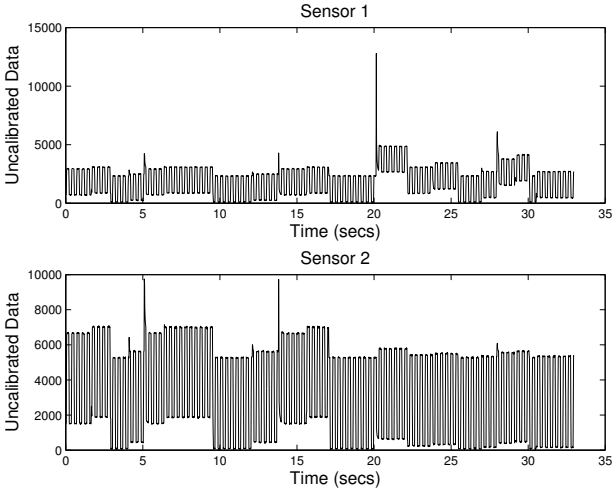

(b) Calibrating load connected to phase B

Fig. 18. WattsWorth sensors responding to calibration load on each phase

following definition of a 3Hz square wave sampled at 60Hz,

$$f_{sq}[n] = \text{sgn}(\sin(n\frac{2\pi}{20})) \tag{12}$$

the calibration signal can be expressed as:

$$f_{prep}[n] = Sf_{sq} \tag{13}$$

where S is an unknown scale factor representing the sensor's response to the calibration load. Leveraging the orthogonality of sinusoids and assuming the calibration load is the dominant current draw at 3Hz, the known Fourier coefficients of the calibration load are equal to the measured Fourier coefficients of the sensor output.

The Discrete Fourier Transform (DFT) is defined as

$$\hat{x}[k] = \frac{1}{N}\sum_{n=0}^{N-1} x[n]e^{-2\pi j\frac{kn}{N}} \tag{14}$$

Since the DFT is a linear operation the transform of the measured signal is:

$$\hat{f}_{prep}[k] = S\mathcal{F}\{f_{sq}\} \tag{15}$$

Taking the transform of 200 samples, the 3Hz fundamental of the calibration waveform appears at $\hat{f}_{prep}[10]$ and $\hat{f}_{prep}[190]$. Because $f_{prep}[n]$ is a real signal the Fourier series is symmetric so the calibration coefficient can be calculated using a single term.

$$\begin{aligned}\hat{f}_{prep}[10] &= S\frac{1}{200}\sum_{n=0}^{199} f_{sq}[n]e^{-2\pi j\frac{10n}{200}} \\ &= S\frac{2}{\pi}\end{aligned} \tag{16}$$

The calibration load is phase locked to the line voltage by design, so any phase in $\hat{f}_{prep}[10]$ is an artifact of the discrete sampling interval. Taking the magnitude, $|\hat{f}_{prep}[10]|$, corresponds to aligning the sampling interval to a zero crossing in the line voltage. Rearranging the terms to solve for S yields:

$$S = \frac{\pi}{2}|\hat{f}_{prep}[10]| \tag{17}$$

Placing the calculated S values and known calibration load I_{cal} in the fit matrix equation produces the following where the notation S_{xy} denotes the x^{th} sensor's response to the calibration load on phase y:

$$\begin{aligned}\begin{bmatrix} I_{cal} \\ 0 \end{bmatrix} &= \begin{bmatrix} K_{11} & K_{12} \\ K_{21} & K_{22} \end{bmatrix} \times \begin{bmatrix} S_{1A} \\ S_{2A} \end{bmatrix} \\ \begin{bmatrix} 0 \\ I_{cal} \end{bmatrix} &= \begin{bmatrix} K_{11} & K_{12} \\ K_{21} & K_{22} \end{bmatrix} \times \begin{bmatrix} S_{1B} \\ S_{2B} \end{bmatrix}\end{aligned} \tag{18}$$

This represents four linearly independent equations which can be used to solve for the unknown K's. Rearranging the matrices produces:

$$\begin{aligned}\begin{bmatrix} I_{cal} \\ 0 \end{bmatrix} &= \begin{bmatrix} S_{1A} & S_{2A} \\ S_{1B} & S_{2B} \end{bmatrix} \times \begin{bmatrix} K_{11} \\ K_{12} \end{bmatrix} \\ \begin{bmatrix} 0 \\ I_{cal} \end{bmatrix} &= \begin{bmatrix} S_{1A} & S_{2A} \\ S_{1B} & S_{2B} \end{bmatrix} \times \begin{bmatrix} K_{21} \\ K_{22} \end{bmatrix}\end{aligned} \tag{19}$$

These systems can then be solved to find the K's. Figure 19 shows the calibrated sensor response which fully decouples and correctly scales each phase. While this example explicitly solves a two phase system, this technique can be extended to solve systems with any number of conductors and/or phases.

To more efficiently compute the fit matrix in a multi-conductor system, calibration loads can be connected to each phase and run simultaneously. This is advantageous when multiple phases are available at a single point such as the 240V dryer outlets in residential environments and three phase outlets in industrial environments. Simultaneous calibration requires that each load toggle at a distinct frequency such as 0.5Hz, 3Hz, and 7Hz so that the Fourier coefficients of the fundamentals do not interfere and their harmonics do not overlap.

B. Voltage Sensor Calibration

Voltage waveforms are generally less dynamic than current waveforms because the utility is expected to provide a stiff voltage independent of connected loads. The most important aspect of the voltage is its phase which defines whether the measured current corresponds to real or reactive power

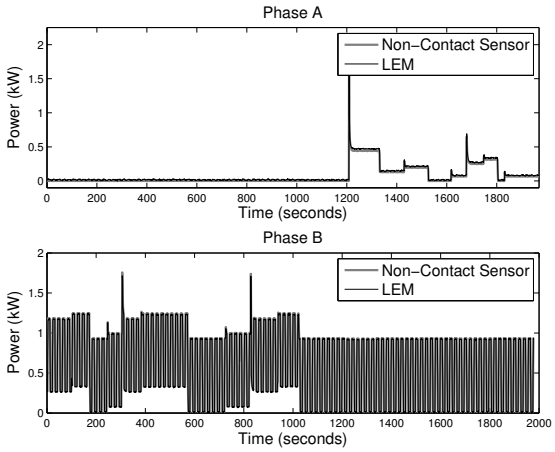

(a) Calibrating load connected to phase A

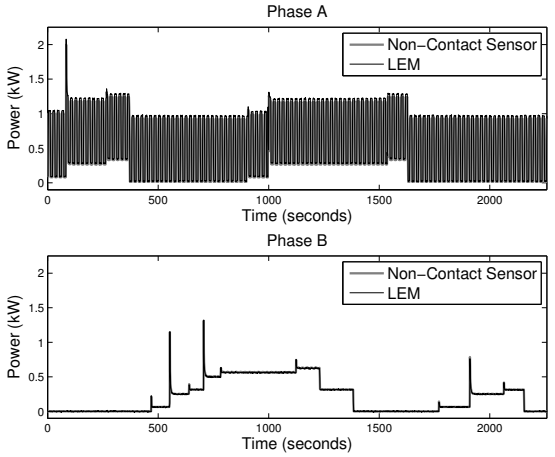

(b) Calibrating load connected to phase B

Fig. 19. WattsWorth sensors displaying correct power consumption after calibration

draw. The techniques described in this section accurately calibrate voltage phase. If the voltage is in fact a function of the connected loads and its precise behavior is important to measure, the previously discussed technique for calibrating currents can be applied to the voltage waveform and a similar set of computations will produce a voltage fit matrix.

In single phase systems, the voltage waveform can be calibrated by scaling the rms output of the sensor directly to the utility's nominal rms voltage. This technique will work well even if the voltage is not stiff, as long as the average rms is a known constant and the calibration window is much longer than any expected ripple in the line. For split phase systems such as residential connections the same technique can be applied because the subspace is one dimensional. A single voltage sensor placed anywhere on the cable or panel will produce a waveform that can be scaled to the correct value of one phase from which the second phase can be recovered with a 180 degree rotation (negation).

In three (or more) phase systems, calibration is more complex because the waveforms span a two dimensional subspace. The electric field can have arbitrary phase depending on the relative contributions of each line phase to the field. In such systems the calibration load provides the required information to recover the line phases. The calibration load is configured to turn on at a positive zero crossing and off at a negative zero crossing and so is perfectly in phase with the line voltage. This means the fundamental of the calibration load current will have the same phase as the line voltage. The phase offset, ϕ is the difference between the fundamental of the calibration load current and the measured voltage phase for the same sampling interval.

$$\phi = \angle V_{sensor}(60\text{Hz}) - \angle I_{sensor}(3\text{Hz}) \tag{20}$$

Rotating the voltage sensor output by $-\phi$ will recover the correct line voltage phase.

$$V_{true}[n] = e^{-j\phi} V_{sensor}[n] \tag{21}$$

The other phases are additional rotations and can be computed analytically rather than sampled directly by sensors.

VII. Conclusions

WattsWorth sensors provide a combined voltage and current monitoring platform in a form factor that attaches easily to circuit breaker panels, power cables, and other power delivery conductors. Because they do not interfere with the physical infrastructure and do not require any service interruption to install it is expected that this type of technology will enable power monitoring in a wide variety of locations where currently such monitors are logistically or physically difficult to deploy. As demand for cost-effective power monitoring systems continues to grow, nonintrusive sensors like WattsWorth remove a barrier to access.

Acknowledgements

This work was supported by a grant from The Grainger Foundation. Additional support was provided by the Martin Foundation, and a grant from the MIT Energy Initiative. The authors gratefully acknowledge the assistance and advice of Dan Vickery, Christopher Schantz, Al Avestruz, Kawin Surakitbovorn, and Professor James Kirtley.

References

[1] "Residential energy consumption survey," *U.S. Energy Information Administration*, March 2013.
[2] S. M.-S. B. Foster, "Results from recent real-time feedback studies," *American Council for an Energy-Efficient Economy*, vol. Report Number B122, February 2012.
[3] E. J. M. et. al., "Engaging electricity demand," in *MIT Study on the Future of the Electric Grid*. MIT Energy Initiative (MITei), December 2011.
[4] "Declaration on power grid investments," *GO 15, Annual Meeting, New York, USA*, October 2013.
[5] *STJ-340: Four Element Bridge Magnetic Sensor Data Sheet*, Micro Magnetics.
[6] *Allegro 1362 Data Sheet*, Allegro.
[7] M. Julliere, "Tunneling between ferromagnetic films," *Phys. Lett.*, vol. 54A: 225226, 1975.
[8] S. S. P. P. et al., "Giant tunnelling magnetoresistance at room temperature with mgo (100) tunnel barriers," *Nat. Mat.*, vol. 3 (12):862867, 2004.
[9] S. I. et al., "Tunnel magnetoresistance of 604% at 300 k by suppression of ta diffusion in cofeb/mgo/cofeb pseudo-spin-valves annealed at high temperature," *Applied Physics Letters*, vol. 98 (8): 082508, 2008.
[10] B. Hoberman, *The Emergence of Practical MRAM*, Crocus Technologies.